

# Learning Stochastic Reduced Models from Data: A Nonintrusive Approach

M.A. Freitag, J.M. Nicolaus, M. Redmann

July 5, 2024

A nonintrusive model order reduction method for bilinear stochastic differential equations with additive noise is proposed. A reduced order model (ROM) is designed in order to approximate the statistical properties of high-dimensional systems. The drift and diffusion coefficients of the ROM are inferred from state observations by solving appropriate least-squares problems. The closeness of the ROM obtained by the presented approach to the intrusive ROM obtained by the proper orthogonal decomposition (POD) method is investigated. Two generalisations of the snapshot-based dominant subspace construction to the stochastic case are presented. Numerical experiments are provided to compare the developed approach to POD.

**Keywords:** nonintrusive model reduction, data-driven modelling, operator learning, scientific machine learning, stochastic systems

**MSC codes:** 60H10, 60H35, 65C30, 60G51

## 1. Introduction

The numerical solution of (stochastic) partial differential equations (PDE) is ubiquitous throughout many fields in engineering and applied sciences. To obtain a numerical model, a spatial discretisation of the governing PDE, for example by finite differences, can be performed. To achieve high accuracy and resolve small-scale phenomena, the utilised discretisation mesh has to be finely grained, resulting in a numerical model of high dimension and computationally expensive evaluations. In a setting, where such a model has to be evaluated often, for instance, when optimising over a parameter or when a Monte-Carlo simulation is run, the computational complexity might result in a practically infeasible algorithm, due to limited computational resources or time sensitivity in an online setting.

The field of model order reduction (MOR) deals with the construction of surrogate models, that are much cheaper to evaluate. In this paper, the full order model (FOM) is a controlled stochastic differential equation (SDE) with bilinear drift and additive noise. That is, the FOM is of the form

$$dX(t) = \left[ AX(t) + Bu(t) + \sum_{i=1}^m N_i X(t) u_i(t) \right] dt + M dW(t), \quad X(0) = X_0, \quad (1)$$

where  $W(t)$ ,  $t \in [0, T]$ , is a  $d$ -dimensional Wiener process with correlation matrix  $K \in \mathbb{R}^{d \times d}$  and  $u : [0, T] \rightarrow \mathbb{R}^m$  an  $m$ -dimensional integrable deterministic control. The initial condition  $X_0$  is assumed to be either deterministic or a Gaussian random variable. Originating from deterministic systems ( $M \equiv 0$ ), a wide range of reduction techniques has been developed. Based on the accessibility of the FOM operators, these approaches into two categories. On the one hand, intrusive model reduction requires knowledge of the

system operators of the FOM to construct the reduced order model (ROM). A famous projection-based method for the reduction of linear time-invariant systems from a system-theoretic perspective is balanced truncation (BT) [1], which has been recently extended to the stochastic case [2]–[5]. Another well-known and closely related, but data-driven, approach is the proper orthogonal decomposition (POD) method [6]. Given snapshots of the system states of the FOM, the POD method constructs an  $r$ -dimensional subspace  $\mathcal{V}_r \subset \mathbb{R}^n$  as the span of the  $r$  leading left-singular vectors  $v_1, \dots, v_r$  of a snapshot-matrix. The matrix  $V_r = [v_1, \dots, v_r] \in \mathbb{R}^{n \times r}$  is then used to define a projection  $P = V_r V_r^T \in \mathbb{R}^{n \times n}$  onto  $\mathcal{V}_r$ . If the FOM coefficients  $A, N_1, \dots, N_m \in \mathbb{R}^{n \times n}$ ,  $B \in \mathbb{R}^{n \times m}$ ,  $M \in \mathbb{R}^{n \times d}$  and the correlation matrix  $K \in \mathbb{R}^{d \times d}$  are available, performing a Galerkin projection yields

$$dX_r(t) = \left[ A_r X(t) + B_r u(t) + \sum_{i=1}^m N_{r,i} X(t) u_i(t) \right] dt + M_r dW(t), \quad (2)$$

with  $X_r(0) = X_{r,0}$  as the POD-ROM. The projected coefficients and initial condition are defined by  $A_r = V_r^T A V_r \in \mathbb{R}^{r \times r}$ ,  $B_r = V_r^T B \in \mathbb{R}^{r \times m}$ ,  $N_{r,i} = V_r^T N_i V_r \in \mathbb{R}^{r \times r}$  and  $M_r = V_r^T M \in \mathbb{R}^{r \times d}$ , as well as  $X_{r,0} = V_r^T X_0$ . The approximation to the FOM is subsequently obtained by lifting  $X(t) \approx V_r X_r(t)$ ,  $t \in [0, T]$ . A structure preserving extension of POD to stochastic systems has recently been proposed [7]. In the presence of componentwise evaluated nonlinearities, the discrete empirical interpolation method (DEIM) [8], [9] provides a reduction method that can be effectively combined with POD. An optimisation-based intrusive MOR technique is the iterative rational Krylov algorithm (IRKA) that aims to minimise a certain error bound between the FOM and the surrogate model [10]. It has also been generalised to SDEs, see [11].

On the other hand, nonintrusive reduction methods construct a surrogate ROM from data without explicit knowledge of the FOM system operators. Examples of nonintrusive reduction methods include the Loewner framework [12]–[17] and dynamical mode decomposition [18]–[22]. Applied to Equation (1), projection-based nonintrusive MOR methods are interested in finding a subspace  $\mathcal{V}_r$  and ROM

$$d\hat{X}_r(t) = \left[ \hat{A}_r \hat{X}_r(t) + \hat{B}_r u(t) + \sum_{i=1}^m \hat{N}_{r,i} \hat{X}_r(t) u_i(t) \right] dt + \hat{M}_r dW(t), \quad (3)$$

with  $\hat{X}(0) = X_{r,0}$ , such that  $V_r \hat{X}_r(t) \approx X(t)$  as well, however, without explicit access to the FOM coefficients, specifically the drift and diffusion operators  $A, B, N_1, \dots, N_m$  and  $M, K$ , respectively. The recently developed operator inference (OpInf) method [23] provides an approach for ODEs with bilinear terms and nonlinearities of polynomial structure by solving a least squares minimisation problem that fits reduced operators to projected FOM state observations. Extensions to nonlinearities via variable transformations [24]–[26], second order systems [27], as well as the combination with an interpolation method for non-polynomial nonlinearities with analytic form [28], are available. The case of noisy or low-quality data was considered by Uy et al. [29]–[31]. Studies on projection-based and interpolation methods can be found, for instance, in [32]–[34].

The goal of this paper is to establish an OpInf approach for SDEs. This is an enormous challenge, since, in addition, the noise process cannot be observed, i.e., even if a path of the SDE solution is available, we do not know the associated trajectory of the driving process. Therefore, it is not possible to construct pathwise accurate approximations. Instead, our ansatz reproduces the distribution of the FOM state variable. We present the details of this work in several sections. It is structured as follows. Section 2 introduces the grey-box-setting of bilinear SDEs under the influence of additive noise. This means that the structure of the full order SDE is known, but not its coefficients. We only have access to (inexact) full order state observations. Building on the briefly explored distributional properties of the FOM, the inference methods of a reduced drift and diffusion coefficients are constructed. A summary of the developed approach by Algorithm 1 concludes the section. In Section 3, the dominant subspace construction based on snapshots, known from POD, is generalised in two ways. These generalisations arise from the way the snapshot-matrix is constructed. To this end, the *state-snapshot-matrix* and the *moment-snapshot-matrix* are introduced. The respective minimisation problems, concerning the optimal projection, are closely related by construction.

Regarding the respective non-singular values, it is shown that, even for general SDEs, the span of the corresponding left-singular vectors of the moment-snapshot-matrix is always contained in the span of the left-singular vectors of the state-snapshot matrix. Section 4 establishes the closeness of the ROM obtained by the developed approach to the intrusive POD ROM. To this end, it is first proved by Theorem 4 that, under certain mild conditions, the inferred operators converge almost surely to the intrusive POD operators. Theorems 5 and 6 bound the difference of the first and second moment between the ROMs in terms of the distance of the respective ROM operators. Hence, together with the almost sure convergence of the inferred operators, it is guaranteed that the expectation and covariance of the OpInf ROM will converge to the expectation and covariance of the POD ROM under the assumptions of Theorem 4. As the expectation and the covariance fully determine the distribution of the state in our setting, we can hence expect a very good approximation of the FOM statistical properties in case enough data is collected. Section 5 provides three numerical experiments, which compare the developed approach to the POD method. This is done by using the summed relative errors in expectation and covariance, respectively, as well as the relative weak error with respect to two functionals, evaluated at the end-time  $T$ .

## 2. Nonintrusive Model Order Reduction in the SDE setting

In the deterministic case of (1) ( $M \equiv 0$  or  $K \equiv 0$ ), the OpInf approach and the extensions thereof [23]–[31], can provide an effective and easy to implement reduction method that solely requires the accessibility of observations of system-state, input  $u$  and the initial condition. The original method obtains the reduced operators by solving a least-squares-problem, where the right-hand side is constructed from approximated time-derivatives of the state-trajectory at the observation times.

However, the stochastic case poses the challenge that the paths of  $X(t)$ ,  $0 \leq t \leq T$  are not differentiable, thereby prohibiting the application of this method. Furthermore, observations of the noise process  $W$  are usually not available. Hence, a pathwise approximation, also known as strong approximation, is infeasible. Therefore, the proposed method aims to obtain a ROM that approximates the FOM in the weak sense, i.e., that the approximation is with regard to the distribution of the FOM at each time  $t \in [0, T]$ .

A general linear SDE [35] can be solved by utilising the corresponding fundamental matrix. Considering the FOM (1), one can find the explicit solution representation

$$X(t) = \Phi(t) \left( X_0 + \int_0^t \Phi(s)^{-1} B u(s) ds + \int_0^t \Phi(s)^{-1} M dW(s) \right), \quad (4)$$

where  $\Phi(t) \in \mathbb{R}^{n \times n}$  is the fundamental matrix that solves the differential equation

$$\dot{\Phi}(t) = \left[ A + \sum_{i=1}^m N_i u_i(t) \right] \Phi(t), \quad \Phi(0) = I_n.$$

Here,  $I_n$  denotes the identity matrix with  $n$  rows and columns. Since the control  $u$  is chosen to be deterministic, the integral  $\int_0^t \Phi(t)\Phi(s)^{-1} M dW(s)$  can be interpreted in the Wiener sense and is therefore a Gaussian random variable for each time  $t \in [0, T]$ . Hence,  $X(t)$  is also Gaussian and therefore determined, in distribution, by its expectation  $E(t) \in \mathbb{R}^n$  and covariance  $C(t) \in \mathbb{R}^{n \times n}$ . Furthermore, since the ROMs (2) and (3) are of the same structure as SDE (1), the distribution of the reduced variables is Gaussian as well. As mentioned above, observations of  $W$  are generally unavailable. In the remainder of this section, an OpInf method is developed that solely requires samples of observations of the FOM system state, but does not rely on the observations of the paths of  $W$ . As a consequence, the ROM is constructed to approximate the FOM in distribution. In the setting of (1) this equates to approximations  $V_r E_r(t) \approx E(t)$  and  $V_r C_r(t) V_r^T \approx C(t)$  instead of an approximation of the FOM system state, where  $V_r$  is a suitable matrix determining the projection.

**Drift operator inference** Defining  $E(t) := \mathbb{E}[X(t)]$ , one obtains that the dynamics of the FOM expectation are governed by

$$\begin{aligned} E(t) &= E(0) + \int_0^t \mathbb{A}E(s) + \mathbb{B}u(s) + \sum_{i=1}^m \mathbb{N}_i E(s) u_i(s) \, ds \\ \iff \dot{E}(t) &= \mathbb{A}E(t) + \mathbb{B}u(t) + \sum_{i=1}^m \mathbb{N}_i E(t) u_i(t). \end{aligned} \quad (5)$$

The statement is obtained by representing equation (1) in integral form, taking expectations on both sides and exploiting that the Itô integral has mean zero. Note that the noise generating Wiener process  $W$  does not appear in the expectation dynamics. The trajectory of  $E(t), t \in [0, T]$ , is therefore smooth almost everywhere if the control  $u$  is integrable. Similarly, one obtains an ODE of the same structure

$$\dot{E}_r(t) = \mathbb{A}_r E_r(t) + \mathbb{B}_r u(t) + \sum_{i=1}^m \mathbb{N}_{r,i} E_r(t) u_i(t) \quad (6)$$

for the expected value  $E_r(t) = \mathbb{E}[X_r(t)]$  of the POD ROM (2). Following the ideas of deterministic OpInf, let the  $s+1$  observation times between  $t_0 = 0$  and  $t_s = T$  be denoted by  $t_i, i = 0, \dots, s$  and define

$$E_r := [E_r(t_0), \dots, E_r(t_s)] \in \mathbb{R}^{r \times s+1} \quad (7a)$$

$$U := [u(t_0), \dots, u(t_s)] \in \mathbb{R}^{m \times s+1} \quad (7b)$$

$$U \odot E_r := [u(t_0) \otimes E_r(t_0), \dots, u(t_s) \otimes E_r(t_s)] \in \mathbb{R}^{mr \times s+1} \quad (7c)$$

$$D := [E_r^T, U^T, (U \odot E_r)^T]^T \in \mathbb{R}^{(r+m+mr) \times s+1} \quad (7d)$$

$$R := [\dot{E}_r(t_0), \dots, \dot{E}_r(t_s)] \in \mathbb{R}^{r \times s+1}. \quad (7e)$$

Exploiting the affine linear dependence of (6) on  $E_r(t)$  and  $u(t)$ , one can easily see that

$$R = O_r \cdot D,$$

with  $O_r := [\mathbb{A}_r, \mathbb{B}_r, \mathbb{N}_{r,1}, \dots, \mathbb{N}_{r,m}] \in \mathbb{R}^{r \times r+m+mr}$  is satisfied exactly. The OpInf approach now consists of formulating and solving the inverse problem

$$\hat{O}_r = \underset{\tilde{O}_r \in \mathbb{R}^{r \times (r+m+mr)}}{\operatorname{arg\,min}} \quad \|R^T - D^T \tilde{O}_r^T\|_F^2 \quad (8)$$

for  $D$  and  $R$  given, e.g., based on (inexact) observations. By construction, the concatenated POD drift operators  $O_r$  solve (8). Furthermore, if the data-matrix  $D$  has full row-rank, the solution is unique.

However, direct observations of  $\dot{E}_r(t)$  or of  $E_r(t)$  are generally unavailable. Instead, only finitely many samples of the state at discrete times  $t_0 = 0, \dots, t_s = T$  are available. The *state-snapshot-matrix* is defined to be the column-wise arrangement of all  $L$  sampled realisations of the states of (1) at the time steps  $t_0, \dots, t_s$

$$\mathbb{X} := [X(t_0, \omega_1), \dots, X(t_s, \omega_L)] \in \mathbb{R}^{n \times (s+1)L}. \quad (9)$$

Note that the observations  $X(t_i, \omega_j)$  might be obtained by numerical simulations and therefore are samples of the state of time-discretised dynamical system, rather than samples of the time-continuous solution of the FOM SDE. Hence, any approximation of the moments of  $X(t)$  by such observations is influenced by two error sources: the finite number of samples  $L$  and the time-discretisation of the continuous dynamics. The columns  $E_{r,i}^L, i = 0, \dots, s$  of the empirical mean of the projected states

$$E_r^L := [E_{r,0}^L, \dots, E_{r,s}^L], \quad \text{with } E_{r,i}^L = \frac{1}{L} \sum_{j=1}^L V_r^T X(t_i, \omega_j) \quad (10)$$

approximate the trajectory of the expected value  $E_r(t) := \mathbb{E}[X_r(t)]$  at the observation times  $t_0 = 0, \dots, t_s = T$ . The precise choice of the projection matrix  $V_r$  depends on the particular approach that we specify in Section 3. If the time between the observations is sufficiently small, the time derivative of  $\dot{E}_r(t_i)$ ,  $i = 0, \dots, s$  can be approximated from  $E_r^L$ , for example, by a finite difference scheme. The result of such an approximation of  $\dot{E}_r(t)$  at the time  $t = t_i$  is denoted with  $\dot{E}_{r,i}^{L,h}$ . Now, utilising  $E_r^L$  and  $\dot{E}_r^{L,h} := [\dot{E}_{r,0}^{L,h}, \dots, \dot{E}_{r,s}^{L,h}]$ , instead of  $E(t)$  and  $\dot{E}(t)$ , to construct

$$\begin{aligned} \mathbf{D}^{L,h} &= [(E_r^L)^T, \mathbf{U}^T, (\mathbf{U} \odot E_r^L)^T]^T \in \mathbb{R}^{(r+m+mr) \times s+1} \text{ and} \\ \mathbf{R}^{L,h} &:= [\dot{E}_{r,0}^{L,h}, \dots, \dot{E}_{r,s}^{L,h}] \in \mathbb{R}^{r \times s+1}. \end{aligned}$$

One can solve the perturbed version of the least squares problem (8)

$$\hat{\mathbf{O}}_r^{L,h} = \arg \min_{\tilde{\mathbf{O}}_r \in \mathbb{R}^{r \times (r+m+mr)}} \|(\mathbf{R}^{L,h})^T - (\mathbf{D}^{L,h})^T \tilde{\mathbf{O}}_r^T\|_F^2 \quad (11)$$

to obtain an approximation  $\hat{\mathbf{O}}_r^{L,h} = [A_r^{L,h}, B_r^{L,h}, N_{r,1}^{L,h}, \dots, N_{r,m}^{L,h}]$  of  $\hat{\mathbf{O}}_r$ . If one can guarantee that  $\mathbf{D}^{L,h}$  and  $\mathbf{D}$  have full rank, then  $\hat{\mathbf{O}}_r^{L,h}$  is an estimate of  $\mathbf{O}_r$ , since the solutions of (8) and (11) are unique.

**Diffusion operator inference** Similar to before, the time evolution of the covariance matrix  $C(t)$  by is described by a (Lyapunov) differential equation. First, the centred process  $X^C(t) := X(t) - E(t)$  satisfies the SDE

$$dX^C(t) = \left[ AX^C(t) + \sum_{i=1}^m N_i X^C(t) u_i(t) \right] dt + M dW(t).$$

Next, applying Itô's product rule to the product  $X^C(t)X^C(t)^T$  results in

$$\begin{aligned} dX^C(t)X^C(t)^T &= [AX^C(t)X^C(t)^T + X^C(t)X^C(t)^T A^T \\ &\quad + \sum_{i=1}^m N_i u_i(t)X^C(t)X^C(t)^T + \sum_{i=1}^m X^C(t)X^C(t)^T (N_i u_i(t))^T] dt \\ &\quad + M dW(t)X^C(t)^T + X^C(t) dW(t)^T M^T + MKM^T dt. \end{aligned}$$

Again, due to inaccessibility of the noise realisations, expectations are taken on both sides. With  $C(t) := \mathbb{E}[X^C(t)X^C(t)^T]$ , the zero mean of the Itô integral and slight algebraic manipulations, one obtains

$$\frac{d}{dt}C(t) = \Psi(t)C(t) + C(t)\Psi(t)^T + MKM^T,$$

where  $\Psi(t) := A + \sum_{i=1}^m N_i u_i(t)$  and the initial condition is given by  $C(0) = \text{Cov}(X_0)$ , where  $\text{Cov}(\cdot)$  denotes the covariance matrix of a random vector. For the POD ROM one obtains a similar system

$$\frac{d}{dt}C_r(t) = \Psi_r(t)C_r(t) + C_r(t)\Psi_r(t)^T + M_r K M_r^T,$$

with  $\Psi_r(t) := A_r + \sum_{i=1}^m N_{r,i} u_i(t)$  and  $C_r(0) = \text{Cov}(X_{r,0}) = V_r^T \text{Cov}(X_0) V_r$ . The influence of the inhomogeneities  $\mathbf{H} = \mathbf{MKM}^T$  and  $\mathbf{H}_r = M_r \mathbf{K} M_r^T$  on the previous equations is independent of time and the corresponding drift operators. Defining  $S_{r,i}$  as the residual

$$S_{r,i} := \dot{C}_r(t_i) - [\Psi_r(t_i)C_r(t_i) + C_r(t_i)\Psi_r(t_i)^T], \quad (12)$$

the least squares problem

$$\hat{\mathbf{H}}_r = \arg \min_{\tilde{\mathbf{H}} \in \mathbb{R}^{r \times r}} \sum_{i=1}^s \|S_{r,i} - \tilde{\mathbf{H}}\|_F^2 \quad (13)$$

is solved by  $H_r$ . To obtain a practically feasible minimisation problem, the (reduced) empirical covariances

$$C_{r,i}^L := \frac{1}{L-1} \sum_{k=1}^L (V_r^T X(t_i, \omega_k) - E_{r,i}^L)(V_r^T X(t_i, \omega_k) - E_{r,i}^L)^T, \quad i = 0, \dots, s$$

are computed from the collected snapshot data  $\mathbb{X}$  and involve a projection matrix  $V_r$  specified in Section 3. The approximations  $\hat{C}_{r,i}^{L,h}$  of the time derivatives are obtained, for instance, again by a finite difference scheme. Subsequently, a perturbed version

$$\hat{H}_r^{L,h} = \arg \min_{\tilde{H} \in \mathbb{R}^{r \times r}} \sum_{i=1}^s \|S_{r,i}^{L,h} - \tilde{H}\|_F^2, \quad (14)$$

of (13) can be constructed using

$$\begin{aligned} \Psi_{r,j}^{L,h} &:= A_r^{L,h} + \sum_{i=1}^m N_{r,i}^{L,h} u_i(t_j), \\ S_{r,i}^{L,h} &:= \hat{C}_{r,i}^{L,h} - \left[ \Psi_{r,i}^{L,h} C_{r,i}^L + C_{r,i}^L (\Psi_{r,i}^{L,h})^T \right], \end{aligned}$$

solely from the available snapshot data and already inferred drift operators. Finally, to obtain the diffusion coefficient  $\hat{M}_r \in \mathbb{R}^{r \times d_r}$  and covariance matrix  $\hat{K}_r \in \mathbb{R}^{d_r \times d_r}$  from  $\hat{H}_r \in \mathbb{R}^{r \times r}$ , one can choose one of the various matrix factorisation methods, for instance an eigenvalue or square-root free Cholesky decomposition of  $\hat{H}_r$ . Note that the inferred  $\hat{H}_r$  in equation (13) is always of the size of the ROM dimension. This means that the reduced coefficients  $\hat{M}_r$  and  $\hat{K}_r$  provided by the above-mentioned factorisation algorithms are square and of length  $r$ . Therefore, without truncation, the ROM obtained by OpInf requires the sampling of a  $r$ -dimensional Gaussian random variable during the simulation. However, if the original noise dimension  $d$  is smaller than the ROM dimension, it is expected that  $\hat{H}_r^{L,h}$  has eigenvalues close to 0. The simulation of  $r$  dimensional noise is therefore not time efficient. Numerical noise can furthermore lead to the loss of symmetry and negative eigenvalues. In our implementation, we therefore compute an eigenvalue decomposition of

$$\frac{\hat{H}_r^{L,h} + (\hat{H}_r^{L,h})^T}{2} = U_H S_H U_H^T$$

and truncate the columns of  $U_H$  and diagonal entries of  $S_H$  that correspond to eigenvalues less than 0.1% of the maximum eigenvalue. Algorithm 1 summarises the approach detailed above.

---

**Algorithm 1** operator inference for SDE (1)

---

- 1: Collect (inexact) observations  $X(t_0, \omega_j), \dots, X(t_s, \omega_j), j = 1, \dots, L$ .
  - 2: Choose projection matrix  $V_r \in \mathbb{R}^{n \times r}$ .
  - 3: Construct  $D^{L,h}$  and  $R^{L,h}$ .
  - 4: Solve the least squares problem (11) for  $\hat{O}_r^{L,h}$ .
  - 5: Extract system operators  $A_r^{L,h}, B_r^{L,h}, N_{r,1}^{L,h}, \dots, N_{r,m}^{L,h}$  from  $\hat{O}_r^{L,h}$ .
  - 6: Construct  $\Psi_{r,i}^{L,h}$  and  $S_{r,i}^{L,h}$ .
  - 7: Solve least squares problem (14) for  $\hat{H}_r^{L,h}$ .
  - 8: Factorise  $\hat{H}_r^{L,h}$  into  $M_r^{L,h} \in \mathbb{R}^{r \times d_r}$  and  $K_r^{L,h} \in \mathbb{R}^{d_r \times d_r}$ .
  - 9: Return  $A_r^{L,h}, B_r^{L,h}, N_{r,1}^{L,h}, \dots, N_{r,m}^{L,h}, M_r^{L,h}, K_r^{L,h}$ .
- 

### 3. Construction of $\mathcal{V}_r$

This section is concerned with the construction of an orthogonal matrix  $V_r \in \mathbb{R}^{n \times r}$  whose column vectors form a basis of  $\mathcal{V}_r$ . A projection  $P$  onto  $\mathcal{V}_r$  can consequently be defined by  $P = V_r V_r^T \in \mathbb{R}^{n \times n}$ . In the

classical deterministic POD setting, one chooses the subspace  $\mathcal{V}_r$  and the corresponding projection  $\mathbf{P}$  in such a way that  $\mathbf{P}\mathbb{X}$  is the best low-rank approximation of rank  $r$  of the snapshots  $\mathbb{X}$  over all possible subspaces of dimension  $r$ . This corresponds to performing a *principal component analysis* (PCA) on the quadratic form of the snapshots  $\mathbb{X}\mathbb{X}^T \in \mathbb{R}^{n \times n}$ . That is, one computes the leading  $r$  eigenvectors of  $\mathbb{X}\mathbb{X}^T$  onto which the data is subsequently projected. The matrix  $\mathbf{V}_r$  hence consists of the leading  $r$  eigenvectors of  $\mathbb{X}\mathbb{X}^T$  or, equivalently, the leading  $r$  left singular vectors of  $\mathbb{X}$ .

However, to achieve a good approximation in the weak sense of our setting, ideally one could identify a subspace  $\mathcal{V}_r \subset \mathbb{R}^n$  that is simultaneously optimal for the projection of the covariance and expectation, rather than the states of the FOM. To this end, two methods of constructing an appropriate snapshot-matrix are proposed. Both methods retain the interpretability as PCAs, however of different quantities, and reduce to the same POD snapshot matrix in the absence of noise. If one collects the  $L$  independent samples, the immediate generalisation of the POD method suggests collecting the observations into a *state-snapshot-matrix*  $\mathbb{X}$  as defined in (9), or a version thereof with permuted columns. The projection defined by the leading  $r$  left-singular vectors of this state-snapshot-matrix corresponds to a PCA of the over the observation-times averaged non-centralised second moments of  $X(t, \omega)$ ,  $t \in \{t_0, \dots, t_s\}$ . This can be seen by observing that

$$\frac{1}{L-1} \mathbb{X}\mathbb{X}^T = \frac{1}{L-1} \sum_{i=0}^s \sum_{j=1}^L X(t_i, \omega_j) X(t_i, \omega_j)^T \rightarrow \sum_{i=0}^s C(t_i) + E(t_i) E(t_i)^T,$$

for  $L \rightarrow \infty$  by the law of large numbers. Defining  $Z(t) := C(t) + E(t)E(t)^T$  and  $\hat{Z} := \frac{1}{s+1} \sum_{i=0}^s Z(t_i)$ , i.e., the non-centralised quadratic form of  $X(t_i)$  and the average thereof over the observation times, then

$$\frac{1}{(s+1)^2(L-1)^2} \|\mathbb{X}\mathbb{X}^T - \mathbf{P}\mathbb{X}\mathbb{X}^T\mathbf{P}\|_F^2 \rightarrow \|\hat{Z} - \mathbf{P}\hat{Z}\mathbf{P}\|_F^2$$

for  $L \rightarrow \infty$ . Since  $\hat{Z} \in \mathbb{R}^{n \times n}$  is symmetric and positive (semi-)definite, one can compute an eigenvalue decomposition of the form  $\hat{Z} = \mathbf{U}\Sigma\mathbf{U}^T$ , with  $\mathbf{U} \in \mathbb{R}^{n \times n}$  and  $\Sigma = \mathbf{diag}(\lambda_1, \dots, \lambda_n) \in \mathbb{R}^{n \times n}$  where the eigenvalues are ordered according to their magnitude  $\lambda_1 \geq \dots \geq \lambda_n \geq 0$ . It is well known that the solution of minimisation of  $\|\hat{Z} - \mathbf{P}\hat{Z}\mathbf{P}\|_F^2$  over the possible orthogonal projections  $\mathbf{P}$  of rank  $r$  can be obtained by defining  $\mathbf{P}$  as the projection onto the subspace spanned by the  $r$  leading eigenvectors. In particular, this means defining  $\mathcal{V}_r = \text{span}\{u_1, \dots, u_r\}$  and  $\mathbf{P} := [u_1, \dots, u_r]$ , where  $u_r$  is the eigenvector corresponding to the  $r$ -th largest eigenvalue  $\lambda_r$ . The error of this projection then is  $\|\hat{Z} - \mathbf{P}\hat{Z}\mathbf{P}\|_F^2 = \sum_{i=r+1}^n \lambda_i^2$ .

However, since we are interested in the approximation in the weak sense, i.e., in distribution, one could consider a subspace  $\mathcal{V}_r$  that best describes not the states of the FOM system, but the states of expectation  $E(t)$  and covariance  $C(t)$ . To obtain an orthogonal basis for the image space of both functions, one can investigate the column space spanned by the *moment-snapshot-matrix*

$$\mathbf{F} := [E(t_0), \dots, E(t_s), C(t_0), \dots, C(t_s)] = [\mathbf{E}, \mathbf{C}] \in \mathbb{R}^{n \times (n+1)(s+1)}$$

with  $\mathbf{E} = [E(t_0), \dots, E(t_s)] \in \mathbb{R}^{n \times s+1}$  and  $\mathbf{C} = [C(t_0), \dots, C(t_s)] \in \mathbb{R}^{n \times n(s+1)}$ . One can then compute an approximation of the orthogonal basis of the column space of  $\mathbf{F}$  simply by computing the left-singular vectors of the empirical moment-snapshot-matrix

$$\mathbf{F}^L := [\mathbf{E}_{f,0}^L, \dots, \mathbf{E}_{f,s}^L, \mathbf{C}_{f,0}^L, \dots, \mathbf{C}_{f,s}^L] = [\mathbf{E}^L, \mathbf{C}^L] \in \mathbb{R}^{n \times (n+1)(s+1)},$$

where  $\mathbf{E}_{f,i}^L$  and  $\mathbf{C}_{f,i}^L$  are the empirical expectation and covariance of the full-state observations  $X(t_i, \omega_j)$ ,  $j = 1, \dots, L$  at the time  $t_i$ . The matrices  $\mathbf{E}^L \in \mathbb{R}^{n \times s+1}$  and  $\mathbf{C}^L \in \mathbb{R}^{n \times n(s+1)}$  are the respective matrices constructed from the column-wise stacking of the estimated moments. The projection defined by the  $r$  leading left-singular vectors of  $\mathbf{F}^L$  then solves the task of minimising

$$\|\mathbf{F}^L(\mathbf{F}^L)^T - \mathbf{P}\mathbf{F}^L(\mathbf{F}^L)^T\mathbf{P}\|_F^2 = \|\tilde{Z} - \mathbf{P}\tilde{Z}\mathbf{P}\|_F^2,$$

with  $\tilde{Z} = \sum_{i=0}^s \mathbf{E}_{f,i}^L (\mathbf{E}_{f,i}^L)^T + (\mathbf{C}_{f,i}^L)^2$  over all possible orthogonal projections of rank  $r$ . Note, that the quadratic form of the moment-snapshot-matrix is closely related to that of the state-snapshots, with the difference being the omitted scaling by  $(s+1)^{-1}$  and the quadratic appearance of the covariance. The remainder of this section briefly investigates the connection between the left-singular vectors of the snapshot-matrices.

Even outside the presented linear SDE with additive noise setting, it can be established that subspace constructions by the left-singular vectors of the state-snapshots and moment-snapshots are closely related. For the remainder of this section, let the FOM stochastic process  $X(t, \omega) \in \mathbb{R}^n$  be defined by the SDE

$$dX(t) = \mu(t, X(t)) dt + \sigma(t, X(t)) dW(t), \quad t \in [0, T].$$

The coefficient functions  $\mu : [0, T] \times \mathbb{R}^n \rightarrow \mathbb{R}^n$  and  $\sigma : [0, T] \times \mathbb{R}^n \rightarrow \mathbb{R}^{n \times d}$  are nice enough, so that the existence and uniqueness of a global solution  $X$  is guaranteed. Hence, the expectation, and the covariance, defined by  $E(t) := \mathbb{E}[X(t)]$  and  $C(t) := \mathbb{E}[(X(t) - E(t))(X(t) - E(t))^T]$ , exist for all  $t \in [0, T]$ . The restriction to  $t \in [0, T]$  is not necessary and can be replaced by  $t \in [0, \infty)$  without a change in the arguments. The proofs in the remainder of this section make extensive use of the compact SVD (cSVD). That is, any decomposition of a rank  $r_a$  matrix  $A = \mathbf{U}_{r_a} \mathbf{S}_{r_a} \mathbf{V}_{r_a}^T \in \mathbb{R}^{n \times m}$ , such that  $\mathbf{U}_{r_a} \in \mathbb{R}^{n \times r_a}$  and  $\mathbf{V}_{r_a} \in \mathbb{R}^{m \times r_a}$  have orthonormal columns and  $\mathbf{S}_{r_a} \in \mathbb{R}^{r_a \times r_a}$  is a diagonal matrix with the non-zero singular values  $\sigma_1 \geq \dots \geq \sigma_{r_a} > 0$  on the main-diagonal. The following Theorem shows that the space spanned by the left-singular vectors of  $E^L$ , corresponding to non-zero singular values, is a subspace of the left-singular vectors of  $\mathbb{X}$ .

**Theorem 1.** *Let  $L, s \geq 1$  and let the state-snapshot and empirical-expectations-snapshot matrices have the cSVDs*

$$\begin{aligned} \mathbb{X} &= \mathbf{U}_r \mathbf{S}_r \mathbf{V}_r^T \quad \text{and} \\ \mathbf{E}^L &= \mathbf{U}_{e,r_e} \mathbf{S}_{e,r_e} \mathbf{V}_{e,r_e}^T, \end{aligned}$$

respectively. There exists a matrix  $\mathbf{T}_e \in \mathbb{R}^{r \times r_e}$  such that  $\mathbf{U}_{e,r_e} = \mathbf{U}_r \mathbf{T}_e$ .

*Proof.* Without loss of generality, let

$$\mathbb{X} = [X(t_0, \omega_1), \dots, X(t_s, \omega_L)] \in \mathbb{R}^{n \times L(s+1)}$$

be the ordering of the columns of the state-snapshot-matrix. If  $\mathbf{P} \in \mathbb{R}^{L(s+1) \times (s+1)}$  is defined by

$$\mathbf{P} := \frac{1}{L} \mathbf{I}_{s+1} \otimes \mathbb{1}_L,$$

with  $\mathbb{1}_L = [1, \dots, 1]^T \in \mathbb{R}^L$ , then  $\mathbf{E}^L = \mathbb{X} \mathbf{P}$ , since

$$\begin{aligned} \mathbb{X} \mathbf{P} &= \frac{1}{L} [X(t_0, \omega_1), \dots, X(t_0, \omega_L), \dots, X(t_s, \omega_1), \dots, X(t_s, \omega_L)] \cdot (\mathbf{I}_{s+1} \otimes \mathbb{1}_L) \\ &= \frac{1}{L} \left[ \sum_{j=1}^L X(t_0, \omega_j), \dots, \sum_{j=1}^L X(t_s, \omega_j) \right] \\ &= [\mathbf{E}_{f,0}^L, \dots, \mathbf{E}_{f,s}^L]. \end{aligned}$$

Furthermore, by

$$\mathbf{P}^T \mathbf{P} = \frac{1}{L^2} (\mathbf{I}_{s+1} \otimes \mathbb{1}_L^T) \cdot (\mathbf{I}_{s+1} \otimes \mathbb{1}_L) = \frac{1}{L} \mathbf{I}_{s+1},$$

it follows that  $\mathbf{P}$  has orthogonal columns. However, using the  $L \times L$  matrix  $\mathbb{1}_{L \times L}$  with all entries equal to 1, we obtain

$$\mathbf{P} \mathbf{P}^T = \frac{1}{L^2} \mathbf{I}_{s+1} \otimes \mathbb{1}_{L \times L}.$$



Notice that the right-hand-side is only equal to  $\mathbb{I}_{L(s+1)}$  if  $L = 1$ . Exploiting the cSVD  $\mathbb{X} = \mathbf{U}_r \mathbf{S}_r \mathbf{V}_r^T$ , we write

$$\mathbf{E}^L = \mathbb{X} \mathbf{P} = \mathbf{U}_r (L^{-\frac{1}{2}} \mathbf{S}_r) (L^{-\frac{1}{2}} \mathbf{V}_r^T \mathbf{P}),$$

it follows that the computation of  $\mathbf{E}^L$  does not cause any of the non-zero singular values of  $\mathbb{X}$  to vanish. This decomposition is not an SVD, since  $L^{-\frac{1}{2}} \mathbf{V}_r^T \mathbf{P}$  only has orthonormal columns. Let  $\mathbf{E}^L = \mathbf{U}_{e,r_e} \mathbf{S}_{e,r_e} \mathbf{V}_{e,r_e}^T$  be the cSVD of the snapshot-matrix  $\mathbf{E}^L$ . Then,

$$\begin{aligned} \mathbf{E}^L &= \mathbb{X} \mathbf{P}, \\ \iff \mathbf{U}_{e,r_e} \mathbf{S}_{e,r_e} \mathbf{V}_{e,r_e}^T &= \mathbf{U}_r \mathbf{S}_r \mathbf{V}_r^T \mathbf{P}, \\ \implies \mathbf{U}_{e,r_e} &= \mathbf{U}_r \underbrace{\mathbf{S}_r \mathbf{V}_r^T \mathbf{P} \mathbf{V}_{e,r_e} \mathbf{S}_{e,r_e}^{-1}}_{=: \mathbf{T}_e}, \end{aligned}$$

where  $\mathbf{S}_{e,r_e}^{-1} = \text{diag}(\sigma_{e,1}^{-1}, \dots, \sigma_{e,r_e}^{-1})$  is the inverse of  $\mathbf{S}_{e,r_e}$ .  $\square$

Employing similar arguments as in the previous proof, analogous statements regarding the left-singular-vectors of the centralised snapshots and the covariance snapshots can be obtained.

**Lemma 2.** *Let  $L \geq 2$ ,  $s \geq 1$  and let the matrix of empiric-covariance-snapshots have the cSVD  $\mathbf{C}^L = \mathbf{U}_{c,r_c} \mathbf{S}_{c,r_c} \mathbf{V}_{c,r_c}^T$ . There exists a matrix  $\mathbf{T}_c \in \mathbb{R}^{r \times r_c}$ , such that  $\mathbf{U}_{c,r_c} = \mathbf{U}_r \mathbf{T}_c$ .*

*Proof.* Notice that  $\mathbf{C}^L = [\mathbf{C}_{f,0}^L, \dots, \mathbf{C}_{f,s}^L]$  can be written as

$$\mathbf{C}^L = \frac{1}{L-1} \hat{\mathbb{X}} \mathbf{diag}(\hat{\mathbb{X}}_0^T, \dots, \hat{\mathbb{X}}_s^T),$$

where  $\mathbb{X}$  is the matrix of centralised state-snapshots

$$\hat{\mathbb{X}} = [\hat{\mathbb{X}}_0, \dots, \hat{\mathbb{X}}_s] = \mathbb{X} - \mathbf{E}^L \otimes \mathbb{1}_L^T$$

with blocks

$$\hat{\mathbb{X}}_i = [X(t_i, \omega_1) - \mathbf{E}_{f,i}^L, \dots, X(t_i, \omega_L) - \mathbf{E}_{f,i}^L].$$

Now, considering the cSVDs  $\mathbf{C}^L = \mathbf{U}_{c,r_c} \mathbf{S}_{c,r_c} \mathbf{V}_{c,r_c}^T$ ,  $\hat{\mathbb{X}} = \mathbf{U}_{z,r_z} \mathbf{S}_{z,r_z} \mathbf{V}_{z,r_z}^T$  and the previous result, one obtains

$$\begin{aligned} \mathbf{U}_{c,r_c} \mathbf{S}_{c,r_c} \mathbf{V}_{c,r_c}^T &= \mathbf{C}^L \\ &= \frac{1}{L-1} \hat{\mathbb{X}} \mathbf{diag}(\hat{\mathbb{X}}_0^T, \dots, \hat{\mathbb{X}}_s^T) \\ &= \frac{1}{L-1} \mathbf{U}_r (\mathbf{S}_r \mathbf{V}_r^T - \mathbf{T}_e \mathbf{S}_{e,r_e} \mathbf{V}_{e,r_e}^T \otimes \mathbb{1}_L^T) \mathbf{diag}(\hat{\mathbb{X}}_0^T, \dots, \hat{\mathbb{X}}_s^T) \\ \implies \mathbf{U}_{c,r_c} &= \mathbf{U}_r \mathbf{T}_c, \end{aligned}$$

where the transformation matrix  $\mathbf{T}_c$  is

$$\mathbf{T}_c = \frac{1}{L-1} (\mathbf{S}_r \mathbf{V}_r^T - \mathbf{T}_e \mathbf{S}_{e,r_e} \mathbf{V}_{e,r_e}^T \otimes \mathbb{1}_L^T) \mathbf{diag}(\hat{\mathbb{X}}_0^T, \dots, \hat{\mathbb{X}}_s^T) \mathbf{V}_{c,r_c} \mathbf{S}_{c,r_c}^{-1}.$$

$\square$

Collecting the previous results, the following theorem shows that the subspace constructed from the left-singular vectors of  $\mathbb{X}$  is a superset of the subspace obtained from the empiric moment-snapshot-matrix  $\mathbf{F}^L$ .

**Theorem 3.** Let  $L \geq 2$ ,  $s \geq 1$  and let  $\mathbf{U}_{m,r_m} = [u_{m,1}, \dots, u_{m,r_m}] \in \mathbb{R}^{n \times n}$  be the left-singular vectors and  $r_m$  the rank of the empiric moment-snapshot-matrix

$$\mathbf{F}^L = [\mathbf{E}^L, \mathbf{C}^L] = [\mathbf{E}_{f,0}^L, \dots, \mathbf{E}_{f,s}^L, \mathbf{C}_{f,0}^L, \dots, \mathbf{C}_{f,s}^L].$$

The space  $\bar{\mathcal{V}}_{r_m} = \text{span}\{u_{m,1}, \dots, u_{m,r_m}\}$  is a subspace of  $\mathcal{V}_r = \text{span}\{u_1, \dots, u_r\}$  spanned by the left-singular vectors  $\mathbf{U}_r = [u_1, \dots, u_r]$  of the state-snapshot-matrix  $\mathbb{X}$  corresponding to the non-zero singular values.

*Proof.* Similarly to the previous statements, the formulation is equivalent to finding some matrix  $\mathbf{T}_m \in \mathbb{R}^{n \times n}$ , such that  $\mathbf{U}_{m,r_m} = \mathbf{U}_r \mathbf{T}_m$ . Let  $\mathbf{U}_{m,r_m} \mathbf{S}_{m,r_m} \mathbf{V}_{m,r_m}^T$  be a cSVD of the empiric-moment-snapshot-matrix  $\mathbf{F}^L = [\mathbf{E}^L, \mathbf{C}^L]$ . The statement is proven by using the previous results

$$\begin{aligned} \mathbf{U}_{m,r_m} \mathbf{S}_{m,r_m} \mathbf{V}_{m,r_m}^T &= [\mathbf{E}^L, \mathbf{C}^L] \\ &= [\mathbf{U}_{e,r_e} \mathbf{S}_{e,r_e} \mathbf{V}_{e,r_e}^T, \mathbf{U}_{c,r_c} \mathbf{S}_{c,r_c} \mathbf{V}_{c,r_c}^T] \\ &= \mathbf{U}_r [\mathbf{T}_e \mathbf{S}_{e,r_e} \mathbf{V}_{e,r_e}^T, \mathbf{T}_c \mathbf{S}_{c,r_c} \mathbf{V}_{c,r_c}^T] \\ \implies \mathbf{U}_{m,r_m} &= \mathbf{U}_r \mathbf{T}_m, \end{aligned}$$

with

$$\mathbf{T}_m = [\mathbf{T}_e \mathbf{S}_{e,r_e} \mathbf{V}_{e,r_e}^T, \mathbf{T}_c \mathbf{S}_{c,r_c} \mathbf{V}_{c,r_c}^T] \mathbf{V}_{m,r_m} \mathbf{S}_{m,r_m}^{-1}.$$

□

Notice, that for a sufficiently large number of samples, the left-singular vectors of

$$\mathbf{F}^L = [\mathbf{E}_{f,0}^L, \dots, \mathbf{E}_{f,s}^L, \mathbf{C}_{f,0}^L, \dots, \mathbf{C}_{f,s}^L]$$

are approximately the left-singular vectors of  $\mathbf{F} = [\mathbf{E}(t_0), \dots, \mathbf{E}(t_s), \mathbf{C}(t_0), \dots, \mathbf{C}(t_s)]$ . The left-singular vectors of  $\mathbb{X}$  therefore provide an adequate basis for the dynamics of expectation and covariance. Hence, obtaining the projection basis from the SVD of  $\mathbb{X}$  is not only numerically advantageous, but also faster and directly available, since the formation of  $\mathbf{E}^L$  and  $\mathbf{C}^L$  is omitted.

## 4. Closeness to the POD ROM

In this section, it is shown that under certain conditions, the ROM obtained by Algorithm 1 is close in distribution to the ROM obtained by POD, since the expected value and the covariance function are well-approximated for a sufficiently large data set. Moreover, we show in Theorem 4 that the error, introduced by the estimation of  $E_r(t_i)$  and  $C_r(t_i)$ , vanishes as the number of samples increases and the time between observations decreases. In the following, let  $\mathbf{D} \in \mathbb{R}^{(r+m+mr) \times (s+1)}$  be the data-matrix,  $\mathbf{R} \in \mathbb{R}^{r \times s+1}$  the corresponding right-hand-side and

$$\mathbf{S} = [\mathbf{S}_{r,0}^T, \dots, \mathbf{S}_{r,s}^T]^T \in \mathbb{R}^{(s+1)r \times r}$$

the stacked matrix of residuals be the data-matrices, defined in (7) and (12), which are used to obtain  $\hat{\mathbf{O}}_r$  and  $\hat{\mathbf{H}}_r$  from Equations (8) and (13), respectively. For this section, it is assumed that the choice of the subspace  $\mathcal{V}_r$  is fixed.

Let  $L$  be the number of independently sampled solution paths from which the observations are collected. In the performed tests, a significant source of errors in the inference steps (11) and (14), was the approximation of the time-derivative to obtain the respective right-hand sides  $\mathbf{R}_{L,h}$  and  $\mathbf{S}_{r,i}^{L,h}$ . Since the empirical mean and covariance converge almost surely with a rate arbitrarily close to  $\frac{1}{2}$  to the true mean and covariance, a large  $L$  is required to obtain satisfactory approximations. The influence of the noise is especially relevant in

the perturbation of the right-hand side  $R_{L,h}$ . Suppose the (time-continuous) noisy observations of the, for simplicity scalar, expectation are given by  $f(t) = E(t) + \epsilon(t)$ , where the noise is Gaussian  $\epsilon(t) \sim \mathcal{N}(0, \sigma^2(t))$ . The result of a finite difference approximation

$$\frac{f(t+h) - f(t)}{h} = \frac{E(t+h) - E(t)}{h} + \frac{\epsilon(t+h) - \epsilon(t)}{h}$$

is then influenced by the pure-noise term  $\hat{\epsilon}(t, h) = \epsilon(t+h) - \epsilon(t) \sim \mathcal{N}(0, \hat{\sigma}(t, h))$ . If one assumes that  $\epsilon(t+h)$  and  $\epsilon(t)$  are independent for any  $h > 0$  and the variance function  $\sigma$  is continuous, then the variance of  $\frac{1}{h}\hat{\epsilon}(t, h)$  is then given by  $\frac{\hat{\sigma}(t, h)}{h^2} = \frac{\sigma^2(t) + \sigma^2(t+h)}{h^2}$ . Taking the limit  $h \rightarrow 0$  then causes the variance of the  $\frac{1}{h}\hat{\epsilon}(t, h)$  to diverge. Thus, decreasing the time between observations  $h$ , without decreasing the variance in observations appropriately, leads to a dominance of the noise. To avoid this, the distance between observations  $h_L$  needs to be chosen according to the magnitude of the noise and the number of samples  $L$ . For the ease of notation, the time between observations is denoted with  $h = h_L$ . It is furthermore required that the scheme, with which the time derivatives are approximated, converges to the true values for  $h = h_L \rightarrow 0$ , as  $L \rightarrow \infty$ .

**Theorem 4.** Let  $D^{L,h} = D + \Delta D_{L,h}$ ,  $R^{L,h} = R + \Delta R_{L,h}$  and  $S^{L,h} = S + \Delta S_{L,h}$  be the non-zero (perturbed) matrices used to obtain estimates  $\hat{O}_r^{L,h}$  and  $\hat{H}_r^{L,h}$  of  $\hat{O}_r$ ,  $\hat{H}_r$ . Let  $D^T$  have full column rank and let  $h = h_L \rightarrow 0$  as  $L \rightarrow \infty$ , such that the derivative approximation scheme converges. If  $D^{L,h} \rightarrow D$ ,  $R^{L,h} \rightarrow R$  and  $S^{L,h} \rightarrow S$  for  $L \rightarrow \infty$  almost surely, i.e.,

$$P(\lim_{L \rightarrow \infty} \|\Delta D_{L,h}\|_2 = 0) = 1 \quad (15a)$$

$$P(\lim_{L \rightarrow \infty} \|\Delta R_{L,h}\|_2 = 0) = 1 \quad (15b)$$

$$P(\lim_{L \rightarrow \infty} \|\Delta K_{L,h}\|_2 = 0) = 1, \quad (15c)$$

then  $\hat{O}_r^{L,h}$  and  $\hat{H}_r^{L,h}$  converge almost surely to  $\hat{O}_r$  and  $\hat{H}_r$  as  $L \rightarrow \infty$ , i.e.,

$$P(\lim_{L \rightarrow \infty} \|\hat{O}_r^{L,h} - \hat{O}_r\|_2 = 0) = 1, \quad P(\lim_{L \rightarrow \infty} \|\hat{H}_r^{L,h} - \hat{H}_r\|_2 = 0) = 1$$

*Proof.*

The perturbed minimisation problem can be regarded columnwise by

$$\hat{O}_{r,i}^{L,h} = \arg \min_{\tilde{O}_i \in \mathbb{R}^{r+m+mr}} \|(D + \Delta D_{L,h})^T \tilde{O}_{r,i} - (R + \Delta R_{L,h})_i^T\|_2.$$

Due to (15a) it holds that  $\|\Delta D_{L,h}\| < \sigma_{r+m+mr}(D)$  with probability 1 in the limit of  $L \rightarrow \infty$  and  $h$  sufficiently small. That is, the norm of the perturbation is smaller than the smallest singular value of  $D$ . Thus,  $D + \Delta D_{L,h}$  is of full rank in the limit of  $L \rightarrow \infty$ . Perturbation analysis of the full rank least squares problem [36, Theorem 5.3.1] then reveals that the relative error between  $\hat{O}_{r,i}$  and  $\hat{O}_{r,i}^{L,h}$  can be bounded by

$$\frac{\|\hat{O}_{r,i} - \hat{O}_{r,i}^{L,h}\|_2}{\|\hat{O}_{r,i}\|_2} \leq C_i \delta_{L,h} + \mathcal{O}(\delta_{L,h}^2), \quad (16)$$

where  $\delta_{L,h} = \max \left\{ \frac{\|\Delta D_{L,h}\|_2}{\|D\|_2}, \frac{\|\Delta R_{L,h}\|_2}{\|R\|_2} \right\}$  and  $C_i$  is a constant depending on the condition of  $D$  and the angle between  $R_i$  and the residual. Hence, for every column, it holds that

$$\begin{aligned} P\left(\lim_{L \rightarrow \infty} \|\hat{O}_{r,i} - \hat{O}_{r,i}^{L,h}\|_2 = 0\right) &\geq P\left(\lim_{L \rightarrow \infty} \tilde{C}_i \delta_{L,h} + \mathcal{O}(\delta_{L,h}^2) = 0\right) \\ &\geq P\left(\lim_{L \rightarrow \infty} \max \left\{ \frac{\|\Delta D_{L,h}\|_2}{\|D\|_2}, \frac{\|\Delta R_{L,h}\|_2}{\|R\|_2} \right\} = 0\right) \\ &= 1, \end{aligned}$$

with  $\tilde{C}_i = C_i \|\hat{O}_{r,i}\|_2$ . Since the statement holds for every column  $\hat{O}_{r,i}^{L,h}$ , the matrix  $\hat{O}_r^{L,h}$  must converge to  $O_r$  almost surely for  $L \rightarrow \infty$  as well, i.e.,

$$\mathbb{P}(\lim_{L \rightarrow \infty} \|\hat{O}_r^{L,h} - \hat{O}_r\|_2 = 0) = 1.$$

The almost sure convergence of  $\hat{H}_r^{L,h}$  to  $\hat{H}_r$  follows by similar arguments.  $\square$

Theorem 4 tells us that the more data we collect to estimate the mean  $E$  and the covariance  $C$ , the closer we are to the ROM coefficients when being able to observe  $E$  and  $C$  directly.

Before concluding the closeness of the ROM obtained by the presented approach to the POD ROM, the continuity of the expectation and covariance with respect to the initial condition and the ROM coefficients needs to be established. The version of the Gronwall lemma referred to in the proofs of the following theorems is provided in the appendix by Lemma 7.

**Theorem 5.**

Let  $C$  and  $\hat{C}$  be the solutions of the Lyapunov differential equations

$$\begin{aligned} \dot{C}(t) &= \Psi(t)C(t) + C(t)\Psi(t)^T + H(t), & C(0) &= C_0, \\ \dot{\hat{C}}(t) &= \hat{\Psi}(t)\hat{C}(t) + \hat{C}(t)\hat{\Psi}(t)^T + \hat{H}(t), & \hat{C}(0) &= \hat{C}_0, \end{aligned}$$

with coefficients  $H, \hat{H}, \Psi, \hat{\Psi} \in L^1([0, T], \mathbb{R}^{n \times n})$  and let the difference of the coefficient functions be denoted by  $\Delta\Psi = \hat{\Psi} - \Psi$  and  $\Delta H = \hat{H} - H$ . Define  $\Delta C := \hat{C} - C$  and  $e_{cov} = \|\Delta C\|$ . There exist constants  $\alpha_c = \alpha_c(T), \beta_c = \beta_c(T), \gamma_c = \gamma_c(T) > 0$  depending on the end-time  $T, C_0, H$  and  $\Psi$ , such that

$$e_{cov}(t) \leq \left( \alpha_c + \beta_c \int_0^t \|\Delta\Psi(s)\| ds + \gamma_c \int_0^t \|\Delta H(s)\| ds \right) \exp\left( \int_0^t \|\Delta\Psi(s)\| ds \right)$$

for all  $t \in [0, T]$ .

*Proof.* By the Carathéodory existence theorem [37, Theorem 1.45], the unique functions  $C$  and  $\hat{C}$  exist, are absolutely continuous and fulfil their respective Lyapunov differential equations for almost all  $t \in [0, T]$ . From the differential equations of  $C(t)$  and  $\hat{C}(t)$  one obtains the evolution equation of  $\Delta C(t)$

$$\dot{C}_e(t) = \hat{\Psi}(t)\hat{C}(t) + \hat{C}(t)\hat{\Psi}(t)^T + \hat{H}(t) - [\Psi(t)C(t) + C(t)\Psi(t)^T + H(t)]$$

with initial condition  $\Delta C(0) = \hat{C}_0 - C_0$ . Substituting  $\hat{C}(t) = \Delta C(t) + C(t)$ , yields

$$\begin{aligned} \dot{C}_e(t) &= \hat{\Psi}(t)(\Delta C(t) + C(t)) + (\Delta C(t) + C(t))\hat{\Psi}(t)^T + \hat{H}(t) \\ &\quad - [\Psi(t)C(t) + C(t)\Psi(t)^T + H(t)] \\ &= \hat{\Psi}(t)\Delta C(t) + \Delta C(t)\hat{\Psi}(t)^T + \Xi(t), \end{aligned}$$

with

$$\Xi(t) = \Delta\Psi(t)C(t) + C(t)\Delta\Psi(t)^T + \Delta H(t).$$

Switching to the integral representations,  $\Delta C(t)$  satisfies

$$\Delta C(t) = \Delta C(0) + \int_0^t \hat{\Psi}(s)\Delta C(s) + \Delta C(s)\hat{\Psi}(s)^T + \Xi(s) ds$$

and the norm of  $\Delta C(t)$  is bounded by

$$e_{cov}(t) \leq \underbrace{e_{cov}(0)}_{=:\alpha(t)} + \int_0^t \|\Xi(s)\| ds + \int_0^t \underbrace{2\|\hat{\Psi}(s)\|}_{=:\beta(s)} e_{cov}(s) ds.$$

The fundamental theorem of calculus for Lebesgue integrals [38] states that  $a$  is absolutely continuous. Furthermore,  $e_{cov}$  is continuous, since  $C$  and  $\hat{C}$  are continuous. Including the fact that the product of a continuous function and an integrable function over a compact interval is integrable again, the assumptions of the Gronwall lemma 7 are satisfied. Together with the triangle inequality, one obtains explicit bounds for all  $t \in [0, T]$

$$\begin{aligned} e_{cov}(t) &\leq \alpha(t) \exp\left(\int_0^t \beta(s) ds\right) \\ &= \left(e_{cov}(0) + \int_0^t \|\Xi(s)\| ds\right) \exp\left(\int_0^t 2\|\hat{\Psi}(s)\| ds\right) \\ &\leq \left(e_{cov}(0) + \int_0^t 2\|\Delta\Psi(s)\| \|C(s)\| + \|\Delta H(s)\| ds\right) \\ &\quad \cdot \exp\left(\int_0^t \|\Psi(s)\| + \|\Delta\Psi(s)\| ds\right), \end{aligned}$$

which becomes

$$e_{cov}(t) \leq \left(\alpha_c + \tilde{\beta}_c \int_0^t \|\Delta\Psi(s)\| ds + \gamma_c \int_0^t \|\Delta H(s)\| ds\right) \exp\left(\int_0^t \|\Delta\Psi(s)\| ds\right)$$

for all  $t \in [0, T]$ , with

$$\alpha_c = \|\hat{C}(0) - C(0)\| \gamma_c, \quad \tilde{\beta}_c = 2\tilde{c}_1 \gamma_c, \quad \gamma_c = e^{\int_0^T \|\Psi(s)\| ds}$$

and  $\tilde{c}_1 = \max_{s \in [0, T]} \|C(s)\|$ . By bounding  $\|C(t)\|$ , one can remove the dependence of  $\tilde{\beta}_c$  on the state  $C(t)$  and obtain constants that depend solely on the coefficient functions and the difference in initial values. Employing the Gronwall lemma 7 on the norm of

$$C(t) = C_0 + \int_0^t \Psi(s)C(s) + C(s)\Psi(s)^T + H(s) ds$$

yields

$$\|C(t)\| \leq \left(\|C_0\| + \int_0^T \|H(s)\| ds\right) \exp\left(2 \int_0^T \|\Psi(s)\| ds\right) =: c_1$$

for all  $0 \leq t \leq T$ . Defining the constant  $\beta_c = 2c_1 \gamma_c$  then completes the proof.  $\square$

**Theorem 6.**

Let  $E$  and  $\hat{E}$  as the solutions of the ODEs

$$\begin{aligned} \dot{E}(t) &= A(t)E(t) + B(t), \quad E(0) = E_0, \\ \dot{\hat{E}}(t) &= \hat{A}(t)\hat{E}(t) + \hat{B}(t), \quad \hat{E}(0) = \hat{E}_0, \end{aligned}$$

with coefficients  $A, \hat{A} \in L^1([0, T], \mathbb{R}^{n \times n})$  and  $B, \hat{B} \in L^1([0, T], \mathbb{R}^n)$ . Let the deviations in the coefficients be defined by  $\Delta A = \hat{A} - A$  and  $\Delta B = \hat{B} - B$  and the difference between the solutions by  $\Delta E = \hat{E} - E$  and  $e_{exp} = \|\Delta E\|$ . There exist constants  $\alpha_e, \beta_e, \gamma_e \geq 0$  depending on the end-time  $T$ ,  $A$  and  $B$ , such that

$$e_{exp}(t) \leq \left(\alpha_e + \beta_e \int_0^t \|\Delta A(s)\| ds + \gamma_e \int_0^t \|\Delta B(s)\| ds\right) \exp\left(\int_0^t \|\Delta A(s)\| ds\right)$$

for all  $t \in [0, T]$ .

*Proof.* The proof follows similar arguments as in Theorem 5. The constants are given by

$$\alpha_e = \|\hat{E}(0) - E(0)\|\gamma_e, \quad \beta_e = c_3\gamma_e, \quad \text{and} \quad \gamma_e = e^{\int_0^T \|A(s)\| ds},$$

where

$$c_3 = \left( E_0 + \int_0^T \|B(s)\| ds \right) \exp \left( \int_0^T \|A(s)\| ds \right).$$

□

In the deterministic case, it was proved [23] that under certain conditions the nonintrusively obtained ROM is close to the intrusive ROM obtained by POD. By Theorems 5 and 6 the distance of two systems of the structure of (2) in the first and second moment can be bounded by the distance of their respective system operators. Given a fixed ROM dimension  $r$ , Theorems 5 and 6 can be applied to this case by choosing

$$\Psi(t) = A_r + \sum_{i=1}^m N_{r,i} u_i(t), \quad \hat{\Psi}(t) = \hat{A}_r^{L,h} + \sum_{i=1}^m \hat{N}_{r,i}^{L,h} u_i(t), \quad H(t) = H_r, \quad \hat{H}(t) = \hat{H}_r^{L,h}$$

and

$$A(t) = \Psi(t), \quad \hat{A}(t) = \hat{\Psi}(t), \quad B(t) = B_r u(t) \quad \hat{B}(t) = \hat{B}_r^{L,h} u(t).$$

Under the conditions of Theorem 4, mainly that  $h = h_L \rightarrow 0$  is sufficiently slow as  $L \rightarrow \infty$  and the data matrix  $D^T$  has full column rank, it can be ensured that the inferred system operators are close to the intrusive operators obtained by POD with probability 1, if a sufficiently large number of samples is used. Generally, the pointwise convergence of the operator difference does not imply that the integral over the norm difference converges to zero as well. However, in this setting, the inferred operators are independent of time and hence, for instance,

$$\begin{aligned} \int_0^t \|\Psi(s) - \hat{\Psi}(s)\| ds &= \int_0^t \|A_r - \hat{A}_r^{L,h} + \sum_{i=1}^m (N_r - \hat{N}_r^{L,h}) u_i(s)\| ds \\ &\leq \|A_r - \hat{A}_r^{L,h}\| t + \sum_{i=1}^m \|N_r - \hat{N}_r^{L,h}\| \int_0^t \|u_i(s)\| ds \\ &\rightarrow 0 \text{ for } L \rightarrow \infty. \end{aligned}$$

Thus, the expectation and covariance of the ROM obtained by OpInf converge almost surely to the expectation and covariance of the POD ROM in the limit of  $L \rightarrow \infty$  as well. Including the fact that the ROMs are Gaussian for each fixed time  $t \in [0, T]$ , it can be concluded that the presented OpInf approach for linear SDEs with additive noise produces a ROM that is close in distribution to the intrusive POD ROM if sufficiently many samples are used.

## 5. Numerical experiments

In the following section, three experiments are presented, with the help of which the developed method is compared against POD. The drift and diffusion operators of the FOM are obtained by appropriate finite difference discretisation of the specified PDEs in the spatial coordinates. Though strictly speaking, the time derivative of a Wiener process does not exist, the diffusion coefficient  $M dW(t)$  of the FOM can be thought of as corresponding to a term  $\sigma(x)\dot{W}(t)$ . This notation is used for the remainder of this section for ease of notation and brevity.

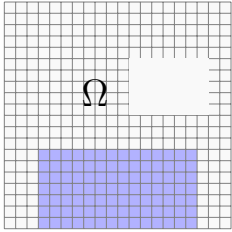
**1d Heat equation** The drift coefficients of the test-model are obtained by spatial discretisation of the one dimensional heat equation with Dirichlet boundary conditions

$$\begin{aligned} \frac{\partial}{\partial t}y - \frac{\partial^2}{\partial x^2}y - \sigma(x)\dot{W}(t) &= 0, \quad x \in (0, 1), t \in (0, 1], \\ y(x, 0) &= y_0 \quad \text{and} \\ y(0, t) = y(1, t) &= u(t), \end{aligned} \tag{17}$$

by finite differences using  $n = 100$  points. In this example, the noise generating Wiener process is of dimension  $d = 2$ . The columns of  $M$  correspond to the evaluation of  $\sigma_1(x) = 0.1 \exp(-10(x - \frac{1}{2})^2)$  and  $\sigma_2(x) = 0.1 \sin(2\pi x)$  on the grid  $x_1, \dots, x_n$ .

**2d Heat equation** This example models the heat spread on the unit square with a hole. The input, modelling the source temperature, is assumed to be noisy and, as such, is modelled by a noisy control  $\tilde{u}(t) = u(t) + 0.1\dot{W}(t)$ . Here,  $u$  is a deterministic function of time which, is perturbed by a  $d = 1$  dimensional Gaussian noise at each time-point  $t$ . The spatial domain, on which the dynamics are defined, is non-convex and the Dirichlet boundary condition is non-continuous at two points of the boundary. The mathematical formulation is given by

$$\begin{aligned} \mathbb{1}_{\Omega_1}(x)\tilde{u}(t) &= \frac{\partial}{\partial t}y(x, t) - \Delta y(x, t), \quad \forall (x, t) \in (\Omega \setminus \Omega_2) \times [0, T] \\ \mathbb{1}_{\partial\Omega_1}(x)\tilde{u}(t) &= y(x, t) \quad \forall (x, t) \in \partial\Omega \times [0, T] \\ 0 &= y(x, t) \quad \forall (x, t) \in \Omega_2 \times [0, T] \\ 0 &= y(x, 0) \quad \forall x \in \Omega, \end{aligned} \tag{18}$$



where the respective domains are specified by  $\Omega = [0, 1]^2$ ,  $\Omega_1 = [0.2, 0.85] \times [0, 0.35]$  and  $\Omega_2 = [0.55, 0.9] \times [0.5, 0.75]$ . The domain  $\Omega \setminus \Omega_2$  was discretised using  $n = 365$  equidistant points. Due to the construction of the example, the matrices  $B \in \mathbb{R}^n$  and  $M \in \mathbb{R}^n$  are identical and consist of only one column. In this setup, the PDE dynamics evolve in a non-convex domain. The Dirichlet boundary condition is piece-wise continuous on  $\partial\Omega$  with non-continuities at  $x \in \{(0.15, 0), (0.85, 0)\}$ .

**Convection reaction equation** This experiment is a modified benchmark problem, which models a convection reaction [39]

$$\frac{\partial}{\partial t}y(t, x, z) = \frac{\partial^2}{\partial x^2}y + \frac{\partial^2}{\partial z^2}y + 20\frac{\partial}{\partial z}y - 180y + F(x, z, t) \tag{19}$$

with vanishing Dirichlet boundary conditions over the unit square. The spatial directions are discretised by a finite difference scheme with 7 and 12 discretisation points, respectively, resulting in a system of dimension  $n = 84$ .<sup>1</sup> The term  $F$  is given by

$$F(y, z, t) = f(y, z)u(t) + \sigma_1(x)\dot{W}_1(t) + \sigma_2(x)\dot{W}_2(t),$$

where the coefficients  $\sigma_1, \sigma_2$  are the same as in Example (17) and the spatial discretisation of  $f(y, z)$  is given by random entries. The FOMs obtained from the described experiments are of the form

$$dX(t, \omega) = [AX(t, \omega) + Bu(t)] dt + M dW(t, \omega), \quad X(0, \omega) = X_0(\omega), \tag{20}$$

<sup>1</sup>The FOM matrices are available at [https://morwiki.mpi-magdeburg.mpg.de/morwiki/index.php/Convection\\_Reaction](https://morwiki.mpi-magdeburg.mpg.de/morwiki/index.php/Convection_Reaction).

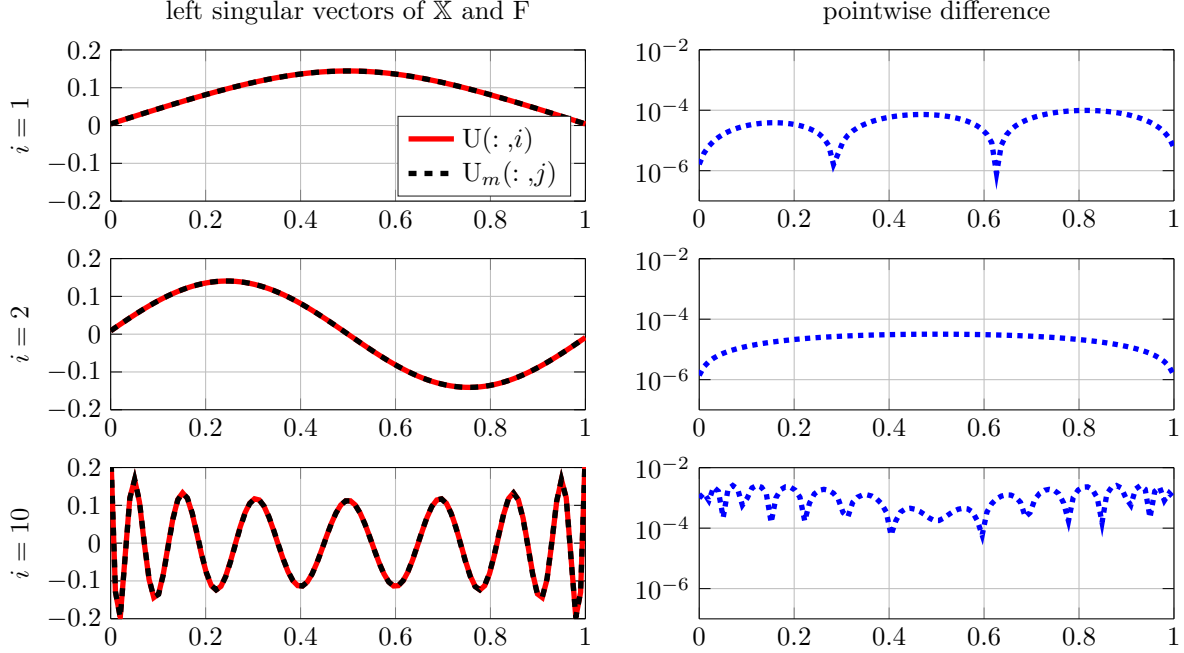


Figure 1: Comparison of left-singular vectors. The vectors  $U(:, i)$  and  $U_m(:, i)$ ,  $i = 1, 2, 10$  are shown in the left column. The right column shows the pointwise absolute difference between the respective vectors.

where  $X(t, \omega) \in \mathbb{R}^n$ ,  $A \in \mathbb{R}^{n \times n}$ ,  $B \in \mathbb{R}^{n \times m}$ ,  $M \in \mathbb{R}^{n \times d}$ , and  $W(t, \omega) \in \mathbb{R}^d$  is a  $d$  dimensional Wiener process. In all examples, the input functions are  $m = 1$  dimensional and the correlation matrices of the noise-generating Wiener processes are the identity  $I_d$ . Figure 1 displays the left-singular vectors of  $\mathbb{X}$  and  $F^L$ , obtained from PDE (17). To this end,  $L = 10^4$  samples of the corresponding FOM were simulated for  $s = 10^3$  time-steps with step-size  $h = 10^{-3}$  using a zero initial condition and input. In this case, the pointwise difference  $U_m(:, i) - U(:, i)$  is less than  $10^{-4}$  for the first pairs of left-singular vectors. The magnitude of this error rises to  $10^{-2}$  for  $i = 10$ . While the plots of Figure 1 in this specific case suggest that the left-singular vectors obtained from the of  $\mathbb{X}$  and  $F^L$  are (almost) identical, this is generally not the case. If, for instance,  $u \equiv 1$  or a polynomial with random coefficients, as in the experiments, is supplied, then the column indices of a subset of left-singular vectors undergo a reordering. Table 1 displays the logarithm of  $\|U_m(:, i) - U(:, j)\|_2$  rounded to two decimals for  $i, j = 1, \dots, 10$ . It is apparent that the fourth, fifth, and sixth left-singular vectors of  $\mathbb{X}$  are the fifth, sixth, and fourth left-singular vectors of  $F^L$ .

Using different initial conditions and inputs [40, Proposition 3.2], the FOM was repeatedly evaluated over  $s = 10^2$  steps with time-step size  $h = 10^{-4}$  to construct a full-rank data-matrix  $D$  with small condition number. To perform the numerical time-integration, a strong drift-implicit Euler-Maruyama scheme [35, Chapter 12.2] was used. The empiric moments used for Algorithm 1 were estimated from  $L = 10000$  sample trajectories, each with identical initial condition and control  $u$ , respectively. The quality of the obtained ROMs is compared using the relative error in expectation, covariance and in the weak sense. Concretely,



i \ j	1	2	3	4	5	6	7	8	9	10
1	<b>-4.06</b>	0.15	0.15	0.15	0.15	0.15	0.15	0.15	0.15	0.15
2	0.15	<b>-3.04</b>	0.15	0.15	0.15	0.15	0.15	0.15	0.15	0.15
3	0.15	0.15	<b>-2.66</b>	0.15	0.15	0.15	0.15	0.15	0.15	0.15
4	0.15	0.15	0.15	0.15	0.15	<b>-2.54</b>	0.15	0.15	0.15	0.15
5	0.15	0.15	0.15	<b>-2.44</b>	0.15	0.15	0.15	0.15	0.15	0.15
6	0.15	0.15	0.15	0.15	<b>-2.26</b>	0.15	0.15	0.15	0.15	0.15
7	0.15	0.15	0.15	0.15	0.14	0.15	<b>-2.23</b>	0.15	0.15	0.15
8	0.15	0.15	0.15	0.15	0.15	0.15	0.14	<b>-2.17</b>	0.15	0.15
9	0.15	0.15	0.15	0.15	0.15	0.15	0.15	0.14	<b>-2.11</b>	0.15
10	0.15	0.15	0.15	0.15	0.15	0.15	0.15	0.15	0.14	<b>-2.05</b>

Table 1: Comparison of the first 10 left-singular vectors obtained from  $\mathbb{X}$  and  $F^L$  for 1d Heat example with zero initial condition and  $u \equiv 1$ . The data was generated using  $L = 10^4$  samples and  $s = 1000$  time-steps of size  $h = 10^{-3}$ . The displayed values are  $\log_{10}(\|U_m(:, i) - U(:, j)\|_2)$  from  $i, j = 1, \dots, 10$  rounded to two decimals.

this means that the following quantities

$$e_E = \frac{\sum_{i=1}^n \|E(t_i) - V_r E_r(t_i)\|_2^2}{\sum_{i=1}^n \|E(t_i)\|_2^2}, \quad (21a)$$

$$e_C = \frac{\sum_{i=1}^n \|C(t_i) - V_r C_r(t_i) V_r^T\|_F^2}{\sum_{i=1}^n \|C(t_i)\|_F^2}, \quad (21b)$$

$$e_{\phi, i}(\tau) = \frac{\|E[\phi_i(X(\tau))] - E[\phi_i(V_r X_r(\tau))]\|}{E[\phi_i(X(\tau))]} \quad \text{for some } 0 \leq \tau \leq T, \quad (21c)$$

were computed for the POD ROM and the ROM obtained by OpInf. The third quantity is called the *relative weak error* of  $X$  with respect to functionals  $\Phi_i : \mathbb{R}^n \rightarrow \mathbb{R}$ , cf. [35]. In the presented error plots of Figure 3, the weak error is measured at the end-time  $\tau = T$ . The functionals

$$\phi_1(\tau) = \|X(\tau)\|_2^2, \quad \text{and} \quad \phi_2(\tau) = \frac{1}{n} \sum_{i=1}^n X_i(\tau)^3 e^{X_i(\tau)} \quad (22)$$

were chosen for the computation of the weak error. While  $\phi_1$  refers to the second moment of  $X(t)$ , the influence of  $X$  on values of  $\phi_2$  is dominated by the large components of  $X$ . The number of samples used for the error computation was set to  $10^6$ . Figures 2 and 3 display the relative errors in the moments and relative weak errors, respectively. Utilising a zero initial condition and a polynomial input, the subspace was constructed from the left-singular-vectors of the empiric moment-snapshot-matrix  $F^L$ , for each example. Choosing the left-singular vectors of state-snapshot-matrix provides similar results. The polynomial was obtained by spline interpolation of 11 equidistantly spaced random values. In all experiments, the approach developed in this work provides ROMs with the same error as POD in the moment approximation until an error level of approximately  $10^{-2}$ , which is the magnitude of the noise contained in the data. With the exception of the 1d Heat equation, reconstruction of the covariance is slightly worse than the approximation in expectation. This is generally to be expected due to the hierarchical structure of inference in Algorithm 1.

Regarding the relative weak error, the estimated results vary by up to two orders of magnitude for each model, depending on the choice of the functional. Again, the noise level in the data used to estimate the ROM operators is reflected in the levelling-off of  $e_{\phi, 1}(T)$  for the OpInf ROM for each experiment. For the 2d Heat equation experiment, a reduced dimension larger than  $r = 5$  does not provide a significant improvement of the approximation properties of the OpInf ROM in any metric. In the cases of the 1d Heat equation and

the convection reaction experiment, errors in expectation and the weak error for  $\phi_1$  level-off after  $r = 5$  as well. However, the error in the covariance and the weak error for  $\phi_2$  continue to decrease until the reduced dimension  $r = 10$ . These results suggest that suitable ROMs of smaller size can be constructed, if one allows some metrics not to be minimized. If, for instance, only the approximation in expectation, but not  $e_C$ , is of interest, then a reduced dimension of  $r = 5$  is sufficient in all the presented examples.

## 6. Conclusion

The inclusion of even a “simple” noise in the system dynamics introduced several new challenges in the OpInf approach, making a direct application of the OpInf method, developed in [23], infeasible. In this paper, a nonintrusive reduced order modelling method was developed that approximates the FOM in the weak sense, i.e., in distribution. It was shown that inferred operators converge almost surely to the POD operators. Together with the continuity of the expectation and covariance of linear SDEs with additive noise with regard to the initial condition and system operators, the closeness of the ROM obtained by the presented approach to the POD ROM was established. Regarding the subspaces spanned left-singular vectors corresponding to non-zero singular values, it was shown that the subspace obtained from the moment-snapshots is always contained in the subspace obtained from the state-snapshots. The numerical experiments demonstrated that the OpInf method produces comparable ROMs to the POD method until the noise-level of the data.

## Reproducibility

The code used in this publication is available at [https://github.com/JMNicolaus/OperatorInference\\_for\\_SDEs](https://github.com/JMNicolaus/OperatorInference_for_SDEs)

## Acknowledgments

The research has been partially funded by the Deutsche Forschungsgemeinschaft (DFG) - Project-ID 318763901 - SFB1294 as well as by the DFG individual grant “Low-order approximations for large-scale problems arising in the context of high-dimensional PDEs and spatially discretized SPDEs” – project number 499366908. In particular, we would like to acknowledge the productive discussions at the annual SFB1294 Spring School 2023. We especially thank Dr. Thomas Mach for the many insightful discussions.

## A. A Gronwall lemma for integrable functions

Various generalisations of the Gronwall lemma have been proposed [41]–[43]. However, most sources only provide statements for continuous coefficients and state the extendability of the results to integrable functions by referencing [44], which is, to our knowledge, unavailable in digital format and not readily accessible. We therefore provide a version of the Gronwall lemma for integrable functions. The proof follows the standard arguments for proving inequalities of this type.

**Lemma 7.** *Let  $\alpha, \beta : [0, T] \rightarrow \mathbb{R}_+$  be real non-negative integrable functions. Furthermore, let  $\alpha$  be non-decreasing. Let  $u \in L^1([0, T])$  be such that*

$$u(t) \leq \alpha(t) + \int_0^t \beta(s)u(s) ds,$$

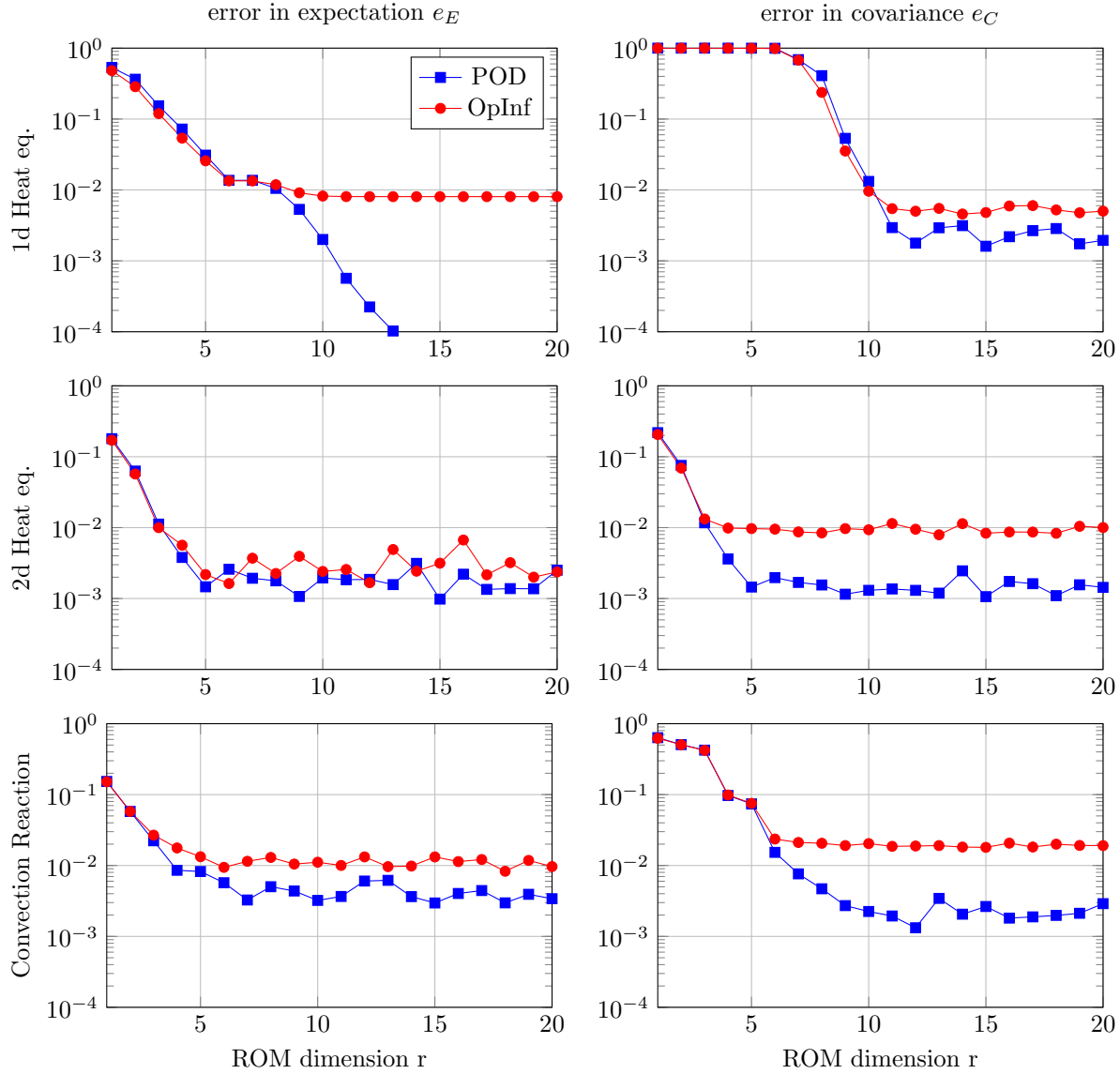


Figure 2: Comparison of POD and OpInf ROMs in expectation and covariance as defined by (21). The data was generated by sampling the FOM  $L = 10^4$  times with  $s = 100$  time-steps of size  $h = 10^{-4}$ . The number of samples for the Monte-Carlo approximation of the errors was  $L = 10^6$ .

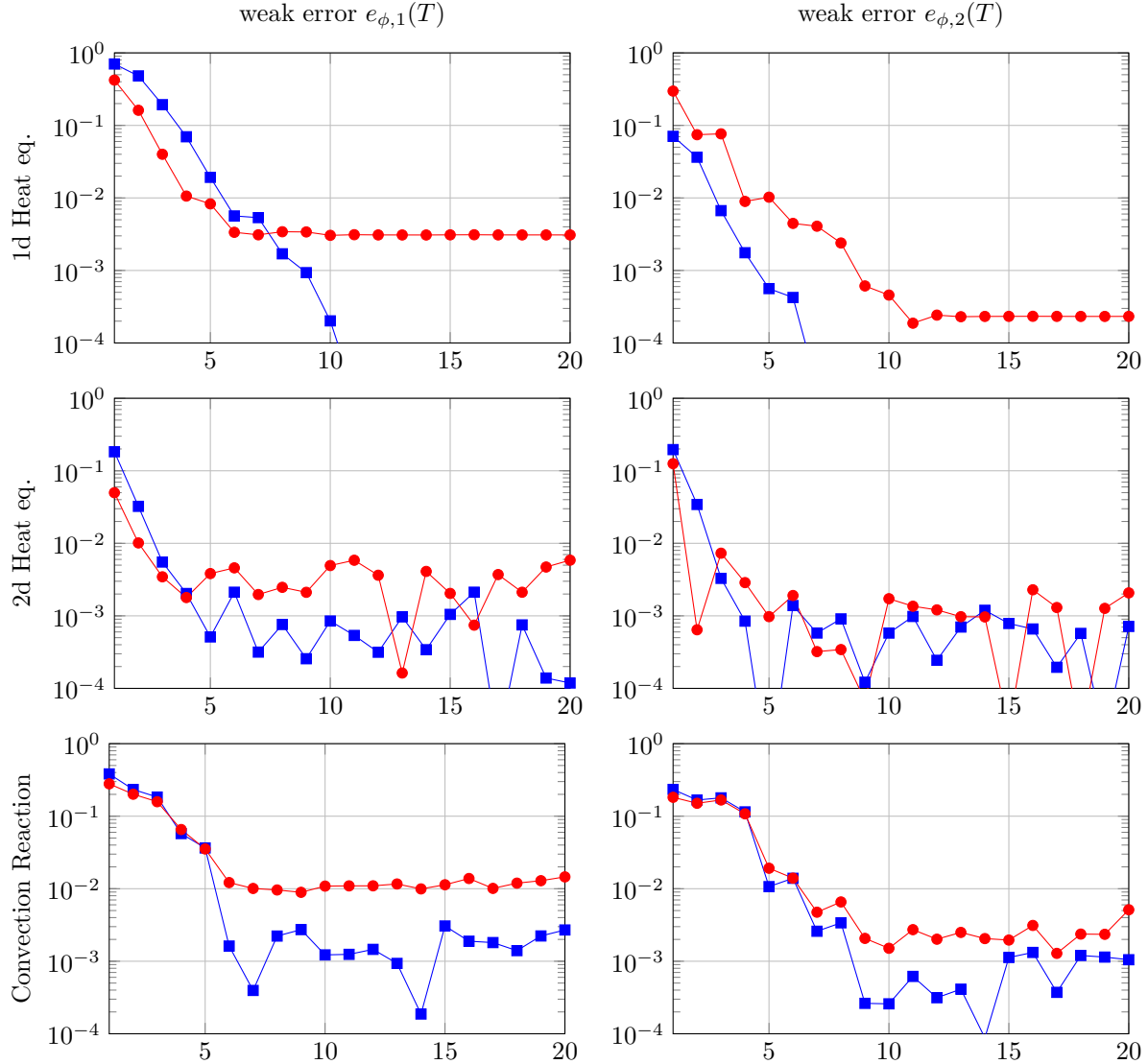


Figure 3: Comparison of POD and OpInf ROMs in the weak error at the end-time point  $\tau = T$  for the functionals  $\phi_1, \phi_2$  (22). The data was generated by sampling the FOM  $L = 10^4$  times with  $s = 100$  time-steps of size  $h = 10^{-4}$ . The number of samples for the error approximation was  $L = 10^6$ .

holds for all  $t \in [0, T]$ . If  $\beta u \in L^1([0, T])$  and  $\beta\alpha \in L^1([0, T])$ , then  $u$  admits to the upper bound

$$u(t) \leq \alpha(t) \exp\left(\int_0^t \beta(s) \, ds\right)$$

for all  $t \in [0, T]$ .

*Proof.* The proof makes extensive use of the fundamental theorem of analysis for the Lebesgue integral [38]. First, since  $\beta \in L^1([0, T])$ , the function  $t \mapsto \int_0^t \beta(s) \, ds$  is absolutely continuous, almost everywhere differentiable and

$$\beta(t) = \left(\int_0^t \beta(s) \, ds\right)'$$

holds almost everywhere. If one defines

$$v(t) = \exp\left(-\int_0^t \beta(s) \, ds\right),$$

then  $v'(t) = -\beta(t)v(t)$  almost everywhere. By the same argument, the integral of  $\beta u$  is absolutely continuous and differentiable almost everywhere. Now, let  $h(t) := v(t) \int_0^t \beta(s)u(s) \, ds$ . Then, by applying the chain rule, it follows that

$$\begin{aligned} h'(t) &= -\beta(t)v(t) \int_0^t \beta(s)u(s) \, ds + v(t)\beta(t)u(t) \\ &= v(t)\beta(t) \left(u(t) - \int_0^t \beta(s)u(s) \, ds\right) \\ &\leq v(t)\beta(t)\alpha(t) \end{aligned}$$

for almost all  $t \in [0, T]$  exploiting the assumption on  $u$ . Since  $v$  is a continuous function and  $\beta\alpha \in L^1([0, T])$ , their product  $v\beta\alpha$  is integrable as well. Hence, by the above inequality, it holds that

$$h(t) = h(t) - h(0) = \int_0^t h'(s) \, ds \leq \int_0^t v(s)\beta(s)\alpha(s) \, ds$$

for all  $t \in [0, T]$ . Dividing by  $v(t)$  and adding  $\alpha(t)$  on both sides leads to

$$u(t) \leq \alpha(t) + \int_0^t \beta(s)u(s) \, ds \leq \alpha(t) + \int_0^t \beta(s)\alpha(s) \frac{v(s)}{v(t)} \, ds$$

for all  $t \in [0, T]$ . Since  $\alpha$  is non-decreasing, the right-hand side can be bounded by

$$\alpha(t) + \int_0^t \beta(s)\alpha(s) \frac{v(s)}{v(t)} \, ds \leq \alpha(t) \exp\left(\int_0^t \beta(s) \, ds\right)$$

for all  $t \in [0, T]$ , completing the proof. □

## References

- [1] B. Moore, “Principal component analysis in linear systems: Controllability, observability, and model reduction,” *IEEE Trans. Automat. Contr.*, vol. 26, 17–32, 1981. DOI: 10.1109/TAC.1981.1102568.
- [2] P. Benner and M. Redmann, “Model reduction for stochastic systems,” *Stoch. Partial Differ. Equ. Anal. Comput.*, vol. 3, 291–338, 2015.

- [3] P. Benner, T. Damm, and Y. R. R. Cruz, “Dual pairs of generalized lyapunov inequalities and balanced truncation of stochastic linear systems,” *IEEE Trans. Autom. Contr.*, vol. 62, 782–791, 2015.
- [4] S. Becker and C. Hartmann, “Infinite-dimensional bilinear and stochastic balanced truncation with explicit error bounds,” *Math. Control Signals Systems*, vol. 31, 1–37, 2019.
- [5] M. Redmann, “Model reduction for stochastic systems with nonlinear drift,” *J. Math. Anal. Appl.*, 128133, 2024. DOI: 10.1016/j.jmaa.2024.128133.
- [6] K. Kunisch and S. Volkwein, “Galerkin proper orthogonal decomposition methods for parabolic problems,” *Numer. Math.*, vol. 90, 117–148, 2001. DOI: 10.1007/s002110100282.
- [7] T. M. Tyranowski, *Data-driven structure-preserving model reduction for stochastic Hamiltonian systems*, 2022. DOI: 10.48550/arXiv.2201.13391.
- [8] S. Chaturantabut and D. C. Sorensen, “Nonlinear model reduction via discrete empirical interpolation,” *SIAM J. Sci. Comput.*, vol. 32, 2737–2764, 2010. DOI: 10.1137/090766498.
- [9] S. Chaturantabut and D. C. Sorensen, “A state space error estimate for POD-DEIM nonlinear model reduction,” *SIAM J. Numer. Anal.*, vol. 50, 46–63, 2012. DOI: 10.1137/110822724.
- [10] S. Güğercin, A. C. Antoulas, and C. Beattie, “ $\mathcal{H}_2$  Model reduction for large-scale linear dynamical systems,” *SIAM J. Matrix Anal. Appl.*, vol. 30, 609–638, 2008. DOI: 10.1137/060666123.
- [11] M. Redmann and M. A. Freitag, “Optimization based model order reduction for stochastic systems,” *Appl. Math. Comput.*, vol. 398, 125783, 2021. DOI: 10.1016/j.amc.2020.125783.
- [12] A. C. Antoulas, I. V. Gosea, and A. C. Ionita, “Model reduction of bilinear systems in the Loewner framework,” *SIAM J. Sci. Comput.*, vol. 38, B889–B916, 2016. DOI: 10.1137/15M1041432.
- [13] A. C. Ionita and A. C. Antoulas, “Data-driven parametrized model reduction in the Loewner framework,” *SIAM J. Sci. Comput.*, vol. 36, A984–A1007, 2014. DOI: 10.1137/130914619.
- [14] J. D. Simard and A. Astolfi, “Nonlinear model reduction in the Loewner framework,” *IEEE Trans. Automat. Contr.*, vol. 66, 5711–5726, 2021. DOI: 10.1109/TAC.2021.3110809.
- [15] J. D. Simard and A. Astolfi, “On the construction and parameterization of interpolants in the Loewner framework,” *Automatica*, vol. 159, 111329, 2024. DOI: 10.1016/j.automatica.2023.111329.
- [16] D. S. Karachalios, I. V. Gosea, and A. C. Antoulas, “On bilinear time-domain identification and reduction in the Loewner framework,” in *Model Reduction of Complex Dynamical Systems*, 2021, 3–30. DOI: 10.1007/978-3-030-72983-7\_1.
- [17] A. J. Mayo and A. C. Antoulas, “A framework for the solution of the generalized realization problem,” *Linear Algebra Appl.*, vol. 425, 634–662, 2007. DOI: 10.1016/j.laa.2007.03.008.
- [18] P. J. Schmid, “Dynamic mode decomposition of numerical and experimental data,” *J. Fluid Mech.*, vol. 656, 5–28, 2010. DOI: 10.1017/S0022112010001217.
- [19] M. O. Williams, I. G. Kevrekidis, and C. W. Rowley, “A data-driven approximation of the Koopman operator: Extending dynamic mode decomposition,” *J. Nonlinear Sci.*, vol. 25, 1307–1346, 2015. DOI: 10.1007/s00332-015-9258-5.
- [20] J. H. Tu, C. W. Rowley, D. M. Luchtenburg, *et al.*, “On dynamic mode decomposition: Theory and applications,” *J. Comput. Dyn.*, vol. 1, 391–421, 2014. DOI: 10.3934/jcd.2014.1.391.
- [21] J. N. Kutz, S. L. Brunton, B. W. Brunton, and J. L. Proctor, *Dynamic Mode Decomposition*. SIAM, 2016. DOI: 10.1137/1.9781611974508.
- [22] C. W. Rowley, I. Mezić, S. Bagheri, P. Schlatter, and D. S. Henningson, “Spectral analysis of nonlinear flows,” *J. Fluid Mech.*, vol. 641, 115–127, 2009. DOI: 10.1017/S0022112009992059.
- [23] B. Peherstorfer and K. Willcox, “Data-driven operator inference for nonintrusive projection-based model reduction,” *Comput. Methods Appl. Mech. Engrg.*, vol. 306, 196–215, 2016. DOI: 10.1016/j.cam.2016.03.025.

- [24] E. Qian, B. Kramer, B. Peherstorfer, and K. Willcox, “Lift & learn: Physics-informed machine learning for large-scale nonlinear dynamical systems,” *Phys. D*, vol. 406, 132401, 2020. DOI: 10.1016/j.physd.2020.132401.
- [25] E. Qian, I.-G. Farcaş, and K. Willcox, “Reduced operator inference for nonlinear partial differential equations,” *SIAM J. Sci. Comput.*, vol. 44, A1934–A1959, 2022. DOI: 10.1137/21M1393972.
- [26] P. Khodabakhshi and K. E. Willcox, “Non-intrusive data-driven model reduction for differential–algebraic equations derived from lifting transformations,” *Comput. Methods Appl. Mech. Engrg.*, vol. 389, 114–296, 2022. DOI: 10.1016/j.cma.2021.114296.
- [27] Y. Filanova, I. Pontes Duff, P. Goyal, and P. Benner, “An operator inference oriented approach for linear mechanical systems,” *Mech. Syst. Signal Process.*, vol. 200, 110620, 2023. DOI: <https://doi.org/10.1016/j.ymsp.2023.110620>.
- [28] P. Benner, P. Goyal, B. Kramer, B. Peherstorfer, and K. Willcox, “Operator inference for non-intrusive model reduction of systems with non-polynomial nonlinear terms,” *Comput. Methods Appl. Mech. Engrg.*, vol. 372, 113433, 2020. DOI: 10.1016/j.cma.2020.113433.
- [29] W. I. T. Uy, D. Hartmann, and B. Peherstorfer, “Operator inference with roll outs for learning reduced models from scarce and low-quality data,” *Comput. Math. Appl.*, vol. 145, 224–239, 2023. DOI: 10.1016/j.camwa.2023.06.012.
- [30] W. I. T. Uy and B. Peherstorfer, “Operator inference of non-Markovian terms for learning reduced models from partially observed state trajectories,” *J. Sci. Comput.*, vol. 88, 91, 2021. DOI: 10.1007/s10915-021-01580-2.
- [31] W. I. T. Uy, Y. Wang, Y. Wen, and B. Peherstorfer, “Active operator inference for learning low-dimensional dynamical-system models from noisy data,” *SIAM J. Sci. Comput.*, vol. 45, A1462–A1490, 2023. DOI: 10.1137/21M1439729.
- [32] P. Benner, S. Güğercin, and K. Willcox, “A survey of projection-based model reduction methods for parametric dynamical systems,” *SIAM Rev.*, vol. 57, 483–531, 2015. DOI: 10.1137/130932715.
- [33] A. C. Antoulas, C. A. Beattie, and S. Güğercin, *Interpolatory methods for model reduction*. SIAM, 2020. DOI: 10.1137/1.9781611976083.ch1.
- [34] P. Benner, M. Ohlberger, A. Cohen, and K. Willcox, *Model reduction and approximation*. SIAM, 2017, vol. 15. DOI: 10.1137/1.9781611974829.
- [35] P. E. Kloeden and E. Platen, *Numerical solution of stochastic differential equations*. Springer-Verlag, Berlin, 1992, vol. 23. DOI: 10.1007/978-3-662-12616-5.
- [36] G. H. Golub and C. F. Van Loan, *Matrix Computations*, Fourth. Johns Hopkins University Press, Baltimore, 2013.
- [37] T. Roubíček, *Nonlinear Partial Differential Equations with Applications*. Springer, 2013, vol. 153. DOI: 10.1007/978-3-0348-0513-1.
- [38] D. L. Cohn, *Measure Theory: Second Edition*. Springer, 2013. DOI: 10.1007/978-1-4614-6956-8.
- [39] Y. Saad, “Projection and deflation method for partial pole assignment in linear state feedback,” *IEEE Trans. Automat. Contr.*, vol. 33, 290–297, 1988. DOI: 10.1109/9.406.
- [40] W. I. T. Uy and B. Peherstorfer, “Probabilistic error estimation for non-intrusive reduced models learned from data of systems governed by linear parabolic partial differential equations,” *ESAIM Math. Model. Numer. Anal.*, vol. 55, 735–761, 2021. DOI: 10.1051/m2an/2021010.
- [41] D. Willett, “A linear generalization of Gronwall’s inequality,” *Proc. Amer. Math. Soc.*, vol. 16, 774–778, 1965. DOI: 10.1090/S0002-9939-1965-0181726-3.
- [42] D. Willett, “Nonlinear vector integral equations as contraction mappings,” *Arch. Rational Mech. Anal.*, vol. 15, 79–86, 1964. DOI: 10.1007/BF00257405.

- [43] B. G. Pachpatte, *Inequalities for differential and integral equations*. Academic Press, Inc., San Diego, CA, 1998, vol. 197.
- [44] P. Beesack, "Gronwall inequalities. carleton math," *Lecture notes*, vol. 11, 1975.